SUPERCAPACITOR MODULE SIZING CONCERNING OPERATIONAL CONSTRAINTS OF THE POWER CONVERTER

Michal Frivaldský[1], Zdeno Biel[2], Marcel Pčola[2], Gabriel Kácsor[2], Marek Franko[2], Juraj Surový[2,*]

[1]Faculty of Electrical Engineering and Information Technologies, University of Zilina, Zilina, Slovakia
[2]EVPU a.s., Nova Dubnica, Slovakia

*E-mail of corresponding author: surovy@evpu.sk

Michal Frivaldský 0000-0001-6138-3103, Marek Franko 0000-0003-1829-6455

Resume

In this paper, the focus is given on the potential use of the supercapacitor component for peak power delivery, required during operation. Potential application use considered here is electric drive for robotic arm motorization. Automatization of industrial and manufacturing processes requires increasing demands on the use of industrial robots. The motion profiles of such system, requires within the operation peak power demand. The supply system can be composed from DC bus power supply, or combined with energy storage system. Combination with proper energy storage component, can improve energy efficiency and provide peak power for the requirements of the system operation. In this paper, design approach for supercapacitor (SC) module is presented for certain motion profile, which is defined by power requirement here. SC module design reflects input to output electrical specifications, while the most optimal configuration is being identified according to SC operation. This approach refers also to the identification of the operational performance of DC-DC bidirectional converter and its proper topological configuration.

Available online: https://doi.org/10.26552/com.C.2023.063

Article info

Received 12 May 2023
Accepted 27 June 2023
Online 30 June 2023

Keywords:

energy storage
supercapacitor
module
bidirectional converter

ISSN 1335-4205 (print version)
ISSN 2585-7878 (online version)

1 Introduction

Energy efficiency and its optimal utilization are coming more and more important, thus representing interesting point of the scientific interest. Energy sources are converted into different forms and partially stored in the grid system for power shaping or peak demand covering. There are various possibilities how to design energy storage system, while hybridization is coming more popular. Here it means, that the use of combination electrochemical cells with various properties are used for potential optimization of the operational scenarios of target application system. Each of the energy storage technology has its properties, which can be recognized also within lifetime or the value of the capacity. Even iron-based electrochemical cells have long operational life and are environmentally friendly, the energy density is not as high as for other perspective technology [1-2]. Research in this field of technology brought development of supercapacitors, which are characterized by long life operation and very high-power density. The usage of SCs as temporary energy storage for regenerative braking is growing [3-6]. The benefits of the SCs are their extended lifetime, high power density, short charge-discharge time, low input resistance, and environmental friendliness. Energy density is not comparable to the conventional and modern electrochemical cells on the other side, therefore combination of these two technologies represents attractive solutions for many applications whose operation scenarios requires the potential use of hybrid energy storage system (HESS) [7-8].

A hybrid energy storage system (HESS), which complements the beneficial qualities of each module, is the combination of the battery and SC. In this configuration, the battery's operating time is increased while the negative effects of current fluctuation are reduced. This is a crucial component for using HESS. Practically the main task of the capacitor is to cover and absorb peak power demands during the system operation. It means, that the design of supercapacitor must meet power profile of the application [9-11].

In this paper the focus is given on the optimal design of supercapacitor module for hybrid energy

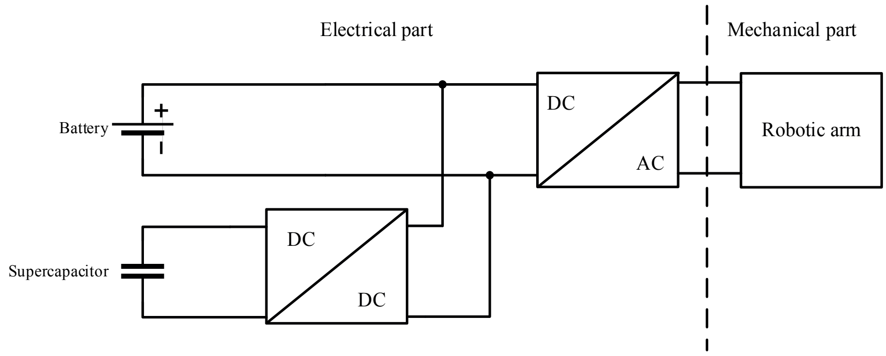

***Figure 1** Block scheme of the electrical and mechanical system*

***Table 1** Input parameter specification*

	Input Parameters		
	Electrical Parameters	minimum	maximum
V_B	Battery voltage	40 V	54.4 V
$V_{SCmodule}$	Supercapacitor voltage	16 V	32 V

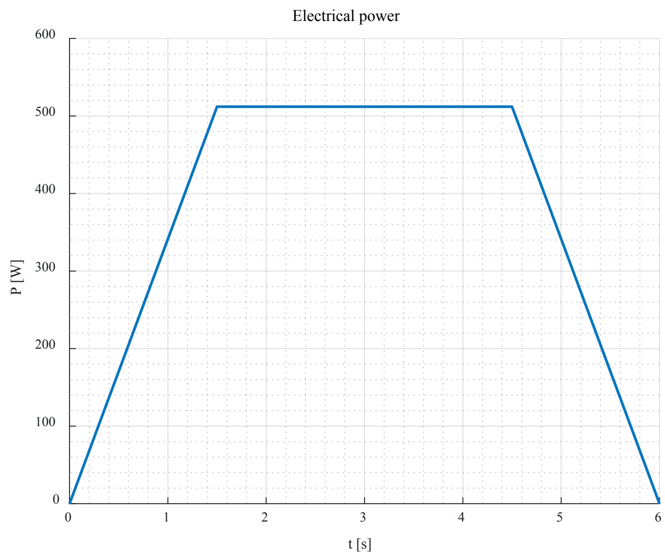

***Figure 2** Time waveform of the power for the working profile (one operational interval)*

supply/storage system. The input to output parameters of the bidirectional DC-DC power converter are defined initially, and are reflecting application properties of HESS. According to the optimization of the supercapacitor module operation, the analysis on the potential topological solution of the DC-DC converter and its duty cycle working range are presented at the end of the paper.

2 System specifications on power electronic circuit

The basic block diagram of the considered system is shown in Figure 1. It consists of a mechanical part, which is formed by a robotic arm, and an electrical part. As a main source is used a battery to maintain a constant power to the load or to charge a supercapacitor. A supercapacitor is used to deliver peak power. The bidirectional DC/DC converter connects the supercapacitor to the battery and to the inverter. The design of supercapacitor bank and selection of a bidirectional DC/DC converter topology is part of the optimization proposal of this paper.

The load is formed by the inverter and the robotic arm. The input parameters for the designing of power converters and supercapacitor bank are stated in a following Table 1.

The voltage of 40 V is for fully discharged and 54.4 V is for fully charged battery pack. The maximum voltage of the V_{SC} supercapacitor is set to 32 V. For efficient utilization of the supercapacitor bank, when

75% of the energy is assumed to be drawn, the minimum voltage value will be half of the maximum. Then the minimum value is 16 V.

The calculation of the supercapacitor capacity C_{SC} depends on the power profile of the load. The power profile is dependent on the working mode of the mechanical movement of the robotic arm. The profile of the mechanical quantities of the working cycle are shown in Figure 2. This cycle corresponds to the specific requirement during the operation of the mechanical system. It is expected here that the power delivery for this time interval (6 seconds) will be covered by the supercapacitor itself. Therefor the design must meets this power requirements.

3 Analysis of supercapacitor module configuration

The power profile specified in Figure 2 is being considered and is used for the determination of the supercapacitor parameters. From Figure 2 is seen that peak power demand is 512 W within 6 s time interval, then steady operation is expected, while required power delivery is supported by the battery system (Figure 1). Based on this, we can calculate the energy that needs to be supplied for a given peak power and will be sourced from supercapacitor module. According to the physical interpretation, the energy is an area covered by time waveform of the power profile. Therefore, when approximation of defined profile (Figure 2), we obtain two triangular time waveforms of power for the duration of 1.5 s and one rectangular waveform lasting for 3 seconds. After the peak power demand, the constant power is delivered to the load. This power is drawn from the battery.

Considering operational and lifetime conditions for the bank of supercapacitor (SC), the key optimization parameters are related to the:

- Maximal current of the supercapacitor cell.
- Ripple current of the supercapacitor cell (during charging and discharging periods).
- Heat dissipation and operational temperature.

The first criterion is affected by the supercapacitor itself, i.e. it is defined by the manufacturer. Optimization regarding maximal current can be later optimized by paralleling cells. Second criterion can be affected by selection of proper converter topology. The third criterion is a matter of design specifications of the supercapacitors bank. These parameters are considered within calculations regarding operational profiles.

Speaking about searching the optimal settings of the bank of supercapacitors, initial focus is given on the possibilities of the ripple current cancelation. Perspective topologies have been developed for this purpose, while interleaving of the power stage of the converter is main approach how to reduce ripple current. From Figure 3 is seen, that with the increase of converter stages, for certain values of the duty cycle, the ripple current reduction is possible.

Presented design approach considers that the sizing of the bank of SC is made in terms of defining the voltage variation during power delivery (Table 1). This operation refers to duty cycle variation during DC-DC converter operation, thus duty cycle range from Figure 3 can be found thus defining the current ripple amplitudes.

Two alternatives are presented here, while it is considered, that during discharging process, after the end of motion profile the voltage on the bank of SC will be 50% from V_{SCmax}. The maximum voltage level V_{SCmax} is 32 V. The voltage at the end of discharging process will be half of the voltage V_{SCmax}, i.e. $V_{SCdisch}$ = 16 V.

The calculation of the energy for the delivering of the peak power to the load is as follows:

A. Calculation based on average power value criterion

The formula for average power calculation considering rectangular waveform is given by next equation:

$$P_{AV} = \frac{1}{T} * P * t\,[W]. \quad (1)$$

For 1st and 3rd interval, triangular waveform is characterized, so the Equation (1) is then modified

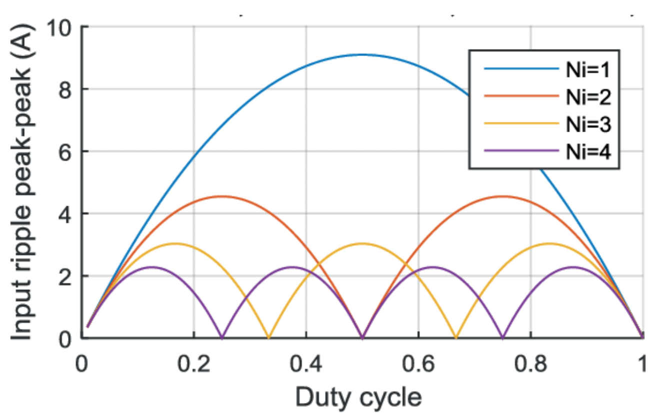

***Figue 3** Magnitude of input ripple as a function of duty cycle for different number of interleaved stages of the DC-DC converter*

***Table 2** Possible SC module configurations*

U_{SC} [V]	C_{SC} [F]	ESR [mΩ]	I_{SCmax} [A]
2.7	5	35	10
2.7	7	31	10
2.7	8	28	12
2.7	10	27	12
2.7	12	26	14
2.7	15	23	17
2.7	20	24	20
2.7	25	20	20
2.7	30	19	25
2.7	35	20	25
2.7	40	18	30
2.7	50	15	30
2.7	60	13	30

$$P_{AVtriangle} = \frac{1}{T} \cdot \frac{P_{peak}}{2} \cdot \frac{T}{4} = \frac{P_{peak}}{8} = 64 \text{ W} . \qquad (2)$$

For 2nd interval (rectangular waveform) the average power is

$$P_{AVconst} = \frac{1}{T} \times P_{peak} \times \frac{T}{2} = \frac{P_{peak}}{2} = 256 \text{ W} . \qquad (3)$$

Then the total power for defined time waveform from Figure 2 is given by Equation (4).

$$P_{AVtot} = 2 \times P_{AVtriangle} + P_{AVconst} = 384 \text{ W} . \qquad (4)$$

Corresponding energy of SC module is then calculated by next formula:

$$E_{SC} = P_{AVtot} \times t = 2304 \text{ J} . \qquad (5)$$

B. Calculation based on energy criterion

Previous procedure considers average power calculation, while in this procedure bit different approach is presented, while it is expected that the results would be the same. General formula for energy calculation is given by Equation (6).

$$E = P \times t \ [\text{J}]. \qquad (6)$$

Then the required energy for 1st and 3rd interval refers to triangular waveform in Equation (7), while rectangular part (2nd interval) of the waveform is characterized by energy requirement described by Equation (8).

$$E_{triangle} = \frac{1}{2} \times P_{peak} * t = \frac{1}{2} \times 512 \times 1.5 = 384 \text{ J} , \qquad (7)$$

$$E_{const} = P_{peak} \times t = 512 \times 3 = 1536 \text{ J} . \qquad (8)$$

Total energy of SC module is:

$$E_{SC} = 2 \times E_{triangle} + E_{const} = 2304 \text{ J} . \qquad (9)$$

Here it is seen, that considering the parameters defined in Table 1, the energy stored within the supercapacitor module must be at least 2304 J.

C. Corresponding capacity of SC module

Continuing design of SC module, the series - parallel configuration targeting properties of the module (energy and voltage) will be analyzed.

$$C_{SC\_module} = \frac{8}{3} \frac{E_{SC}}{V_{SC\max}^2} = \frac{8 * 2304 \text{ J}}{3 * 32^2} = 6 \text{ F} . \qquad (10)$$

According to the current rating of the SC module, the maximum power rating simultaneously with minimal voltage of the module during operation shall be considered. Then for maximal current value, next equation is valid:

$$I_{SC\_moduleMAX} = \frac{P_{peak}}{V_{SC\min}} = \frac{512}{16} = 32 \text{ A} . \qquad (11)$$

D. SC module configuration

Important design issue for supercapacitor module configuration is related to power loss minimization, thus minimization of parasitic ESR of SC module. For prototyping purposes, the SC cell from Vishay series MAL2220 is considered as an example for module configuration. Parameters of single SC cell - series MAL 2220 [12].

Table 2, shows the main parameters of one cell from MAL2220 series, while these are key inputs for SC module configuration, i.e. capacitance, ESR and maximum current of one cell.

To achieve the required voltage of the SC module (32V), it is necessary to configure 12 SC cells in series even any of the component from MAL2220 series is considered. On the other side, if required value of the capacity of SC module (6F) must be met, the situation differs for individual single cell components from Table 2. These variations are summarized in Table 3.

From the available combinations of SC modules

***Table 3** Parameters of different SC modules*

Cell capacity [F]	Nr. of parallel cell	Final capacity [F]	ESR [mΩ]	$I_{SCmoduleMAX}$ [A]
5	15	6.25	28	150
7	11	6.41	33.8	110
8	9	6	37.33	108
10	8	6.66	40.5	96
12	6	6	55.2	84
15	5	6.25	55.2	85
20	4	6.66	72	80
25	3	6.25	80	60
30	3	7.5	76	75
35	3	8.75	80	75
40	2	6.66	108	60
50	2	8.33	90	60
60	2	10	78	60

(Table 3), we consider the SC module solution with the lowest ESR to achieve minimal losses (12S15P with total capacity 6.25F and ESR 28mΩ).

Now, knowing the module configuration, the maximum available energy considering capacity of the module should be recalculated Equation (12) together with minimum available energy calculation referring defined minimal voltage value of SC module in Equation (13). It is a starting point for maximum power loss value identification of the SC module operated under power profile defined by Figure 2.

$$E_{SC\_module\_\max} = \frac{1}{2} \times C \times V_{SC\max}^2 = \frac{1}{2} \times 6.25 \times \times 32^2 = 3200 \text{ J}, \quad (12)$$

$$E_{SC\_module\_min} = \frac{1}{2} \times C \times V_{SCmin}^2 = \frac{1}{2} \times 6.25 \times \times 16^2 = 800 \text{ J}. \quad (13)$$

Because maximum current of SC module will be sourced at minimum voltage value, then considering result from Equation (12) and Equation (9) and by reinterpretation of the capacitor energy formula, the Equation (14) identifies the minimum voltage, which will be reached during module operation under defined power profile.

$$V_{SCmodule_{min}} = \sqrt{\frac{2 \times (E_{SC\_module\_\max} - E_{SC})}{C}} = \sqrt{\frac{2 \times (3200 - 2304)}{6}} = 16.933 \text{ V}. \quad (14)$$

Maximum current of SC module (max power/ voltage of SC module minimal) during operation will be:

$$I_{SC\_module\_MAX} = \frac{P_{peak}}{V_{SC\min}} = \frac{512}{16.933} = 30.24 \text{ A}. \quad (15)$$

The existence of the ESR parameter will reflect within voltage drop of module itself in Equation (17). Calculation of voltage drop considering ESR effect:

$$ESR_{SCmodule} = \frac{Nr_{serial} \times ESR_{1cell}}{Nr_{paralel}} = \frac{12 \times 35\, m\Omega}{15} = 28\, m\Omega, \quad (16)$$

$$\Delta V_{ESR} = ESR_{SCmodule} \times I_{SCmoduleMAX} = 28\, m\Omega \times 30.24 \text{ A} = 0.847 \text{ V}. \quad (17)$$

Now, with regard to evaluated voltage drop reflecting module operation, the minimal voltage on the supercapacitor is given by Equation (18).

$$V_{SCmodule\_\min\_ESR} = V_{SCmodule} \times \Delta V_{ESR} = 16.933 - 0.847 = 16.086\text{V}. \quad (18)$$

Based on this analysis, it is seen, that considering all critical aspects which can affect minimal value of the voltage of SC module, its voltage shall not drop below 16 V.

Finaly power losses can be evaluated using Equation (19).

$$SC_{\text{mod}\_loss} = I_{SC\_module\_MAX}^2 \times ESR_{SCmodule} = 30.24^2 \times 0.028 = 25\text{W}. \quad (19)$$

4 Evaluation of the operational region regarding ripple cancelation of interleaved bidirectional converter

As was mentioned within introductory part of this paper, the use of proper topology of bidirectional converter (Figure 4) may affect operational life of supercapacitor.

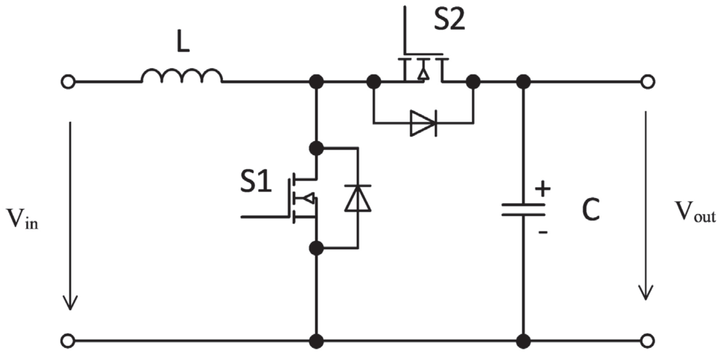

Figure 4 *Principal schematic of bidirectional boost converter*

Table 4 *Defined operational voltage ranges for bidirectional boost converter*

Input/output voltages	Profile 1
$V_{SCmodule}$	32 V - 16.09 V
V_{DCbus}	40 V - 54.4 V

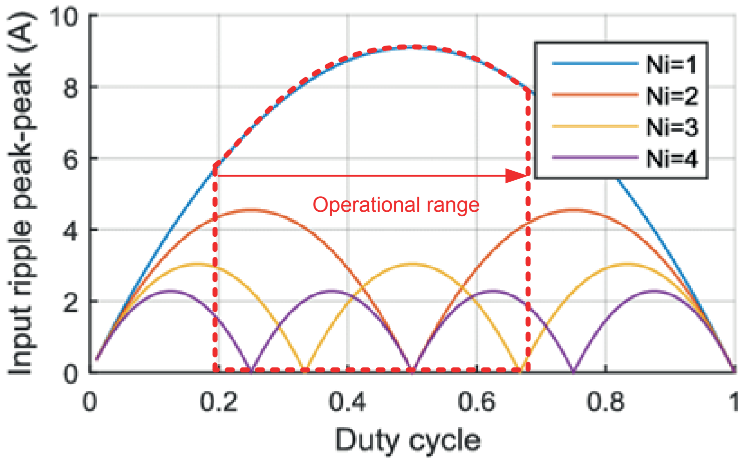

Figure 5 *Operational range of the duty cycle for n-interleaved boost converter*

Interleaved topologies enable to reduce current ripple, which is one of the parameters that markedly affects lifetime of capacitors [13-15]. At this point, the analysis of operational properties of SC module (voltage levels vs. Power demand) will be provided according to duty cycle variation, which results in current ripple cancelation possibilities of interleaved converters (Figure 3). Because DC bus voltage from Figure 1 is higher than voltage of the SC module, the boost topology operation will be considered for bidirectional DC/DC converter.

For the standard boost type of converter (including interleaved), the relationship between input (SC module voltage) to output voltage (DC bus voltage) ratio is defined by duty cycle as follows:

$$\frac{V_{out}}{V_{in}} = \frac{1}{1-D} \rightarrow D = 1 - \frac{V_{in}}{V_{out}}. \tag{20}$$

The operational duty cycle (D) range for boundary states is established. The SC module voltage VSCmodule serves as the boost converter's input voltage, while VDCbus serves as the device's output voltage.

Considering boost mode, the duty cycle can vary within the values, which are affected by the maximum and minimum voltages at the input and output of the converter. For values indicated in Table 4, duty cycle is within interval:

- Low limit of D = from 32 V to 40 V (D = 0.2),
- High limit of D = from 16.09 V to 54.4 V (D = 0.7).

Summarizing achieved results, it is now possible to indicate what would be the ripple current cancelation possibility, when calculated duty cycle values are considered (Figure 5). The results shown below, are clearly indicating that the possibility for SC module operation is possible by using interleaved bidirectional DC-DC converter, while for certain duty cycle range 3-leg and 4-leg represents the best possibility.

5 Conclusion

In this paper, the hybrid energy storage system was introduced as a potential solution for peak power demands. The target application here was focused on possible use of such concept within the electric drive systems for robotic arm motorization. The input to output parameters specification is referring to standard industrial use, while power profile defining the peak demands was defined as well. The main aim of the study was to find optimal solution of design of supercapacitor module, which is responsible for covering energy demands during peak power operation. It refers to proper sizing according to energy, and minimal voltage requirement during discharging process. This is important when we are speaking about effective utilization of supercapacitor module designed from single cells. After energy sizing, the sample part of single cell was defined, while optimal configuration of series and parallel strings have been evaluated according to parasitic resistance reduction. When the proper configuration was selected, the analysis on the operational properties was performed, while power loss generation was calculated as well. Finally, in order to present possible solution to optimize operational performance of the SC module targeting improvements related to operational life, interleaved solution of bidirectional converter have been mentioned in regard to the current ripple reduction on SC module. The analysis of duty cycle operation range was performed and ripple current reduction was represented by the operational characteristics of interleaved bidirectional converters. The study shows several outcomes, i.e. it represents the idea of optimal SC module sizing, while the possibility for lifetime optimization is given as well through duty cycle range identification.

Acknowledgment

This publication was realized with support of Operational Program Integrated Infrastructure 2014 - 2020 of the project: Innovative Solutions for Propulsion, Power and Safety Components of Transport Vehicles, code ITMS 313011V334, co-financed by the European Regional Development Fund.

Conflicts of interest

The authors declare that they have no known competing financial interests or personal relationships that could have appeared to influence the work reported in this paper.

References

[1] SAHIN, M. E., BLAABJERG, F., SANGWONGWANICH, A. A Comprehensive review on supercapacitor applications and developments. *Energies* [online]. 2022, **15**, 674. eISSN 1996-1073. Available from: https://doi.org/10.3390/en15030674

[2] SLADECEK, V., KUCHAR, M., PALACKY, P. LiFePo battery charger with controlled rectifier. In: 18th International Scientific Conference on Electric Power Engineering EPE 2017: proceedings [online]. IEEE. 2017. eISBN 978-1-5090-6406-9. Available from: https://doi.org/10.1109/EPE.2017.7967351

[3] SMITH, S. C., SEN, P. K., KROPOSKI, B. Advancement of energy storage devices and applications in electrical power systems. In: 2008 IEEE Power and Energy Society General Meeting-Conversion and Delivery of Electrical Energy in the 21st Century: proceedings [online]. IEEE. 2008. ISSN 1932-5517, ISBN 978-1-4244-1905-0, p. 1-8. Available from: https://doi.org/10.1109/PES.2008.4596436

[4] LIU, S., WEI, L., WANG, H. Review on the reliability of supercapacitors in energy storage applications. *Applied Energy* [online]. 2020, **278**, 115436. ISSN 0306-2619, eISSN 1872-9118. Available from: https://doi.org/10.1016/j.apenergy.2020.115436

[5] SLADECEK, V., NEBORAK, I., PALACKY, P. Optimisation of electric drive setting in battery-powered locomotive. In: 15th International Scientific Conference on Electric Power Engineering EPE 2014: proceedings [online]. IEEE. 2014. eISBN 978-1-4799-3807-0. Available from: https://doi.org/10.1109/EPE.2014.6839448

[6] PIERSON, J. R., JOHNSON, R. T. The battery designer's challenge - satisfying the ever-increasing demands of vehicle electrical systems. *Journal of Power Sources* [online]. 1991, **33**(1-4), p. 309-318. ISSN 0378-7753, eISSN 1873-2755. Available from: https://doi.org/10.1016/0378-7753(91)85069-9

[7] JING, W., LAI, C.H., WONG, W. S. H., WONG, M. L. D. Battery-supercapacitor hybrid energy storage system in stand-alone DC microgrids: a review. *IET Renewable Power Generation* [online]. 2017, **11**(4), p. 461-469. eISSN 1752-1424. Available from: https://doi.org/10.1049/iet-rpg.2016.0500

[8] SIMCAK, M., SPANIK, P. Comparison of control methods for power stage of battery management systems with 4 cells. In: 21st International Scientific Conference on Electric Power Engineering EPE 2020: proceedings[online]. IEEE. 2020. eISBN 978-1-7281-9479-0. Available from: https://doi.org/10.1109/EPE51172.2020.9269209

[9] CAMARA, M. B., GUALOUS, H., GUSTIN, F., BERTHON, A. Design and new control of DC/DC converters to share energy between supercapacitors and batteries in hybrid vehicles. *IEEE Transactions on Vehicular*

Technology [online]. 2008, **57**(5), p. 2721-2735. ISSN 0018-9545, eISSN 1939-9359. Available from: https://doi.org/10.1109/TVT.2008.915491

[10] VASTA, E., LUCIFORA, A., TORNELLO, L. D., FOTI, S., CACCIATO, M., PERNACI, CH., DE CARO, S., SCELBA, G. State of charge estimation of battery energy storage systems in low voltage electric drive applications for hybrid and electric vehicles. In: 2022 IEEE Energy Conversion Congress and Exposition ECCE: proceedings [online]. IEEE. 2022. eISBN 978-1-7281-9387-8, p. 1-7. Available from: https://doi.org/10.1109/ECCE50734.2022.9947619

[11] VASTA, E., GRECO, D., SCELBA, G., CACCIATO, M., DE BENEDETTI, M. M., LANUZZA, L., EBERHARDT, O., DUGO, D., SAMINARA, G. Design of a battery testing system with software/hardware interface. In: 2022 ELEKTRO: proceedings [online]. IEEE. 2022. eISBN 978-1-6654-6726-1, p. 1-6. Available from: https://doi.org/10.1109/ELEKTRO53996.2022.9803500

[12] Electrical double layer energy storage capacitors power and energy versions - VISHAY, 220 EDLC ENYCAP [online]. Available from: https://www.mouser.com/datasheet/2/427/220edlc_enycap-1762440.pdf

[13] TURZYNSKI, M., BACHMAN, S., JASINSKI, M., PIASECKI, S., RYŁKO, M., CHIU, H.-J., KUO, S.-H., CHANG, Y.-C. Analytical estimation of power losses in a dual active bridge converter controlled with a single-phase shift switching scheme. *Energies* [online]. 2022, **15**, 8262. eISSN 1996-1073. Available from: https://doi.org/10.3390/en15218262

[14] TURZYNSKI, M., CHRZAN, P. J., KOLINCIO, M., BURKIEWICZ, S. Quasi-resonant DC-link voltage inverter with enhanced zero-voltage switching control. In: 2017 19th European Conference on Power Electronics and Applications EPE'17 ECCE Europe: proceedings [online]. IEEE. 2017. eISBN 978-90-75815-27-6, p. P.1-P.8. Available from: https://doi.org/10.23919/EPE17ECCEEurope.2017.8099289

[15] KINDL, V., ZAVREL, M. ,TYRPEKL, M., SIKA, J. Analysis of coupling elements for wireless power transfer with primary side compensation. In: 2022 20th International Conference on Mechatronics - Mechatronika ME: proceedings [online]. IEEE. 2022. eISBN 978-1-6654-1040-3, p. 1-7. Available from: https://doi.org/10.1109/ME54704.2022.9983352